Underfrequency Load Shedding Using Locally Estimated RoCoF of the Center of Inertia

Mingyu Sun ⓘ, *Member, IEEE*, Gaoyuan Liu *, Student Member, IEEE*, Marjan Popov ⓘ, *Senior Member, IEEE*, Vladimir Terzija ⓘ, *Fellow, IEEE*, and Sadegh Azizi ⓘ, *Senior Member, IEEE*

Abstract—The conventional Under Frequency Load Shedding (UFLS) scheme could result in unacceptably low frequency nadirs or overshedding in power systems with volatile inertia. This paper proposes a novel UFLS scheme for modern power systems whose inertia may vary in a wide range due to high penetration of renewable energy sources (RESs). The proposed scheme estimates the rate of change of frequency (RoCoF) of the center of inertia (CoI), and consequently, the loss of generation (LoG) size, using local frequency measurements only. An innovative inflection point detector technique is presented to remove the effect of local frequency oscillations. This enables fast and accurate LoG size calculation, thereby more effective load shedding. The proposed UFLS scheme also accounts for the effect of the inertia change resulting from LoG events. The performance of the proposed scheme is validated by conducting extensive dynamic simulations on the IEEE 39-bus test system using Real Time Digital Simulator (RTDS). Simulation results confirm that the proposed UFLS scheme outperforms the conventional UFLS scheme in terms of both arresting frequency deviations and the amount of load shed.

Index Terms—Center of inertia (CoI), Underfrequency load shedding (UFLS), Rate of change of frequency (RoCoF).

I. INTRODUCTION

THE electrical power industry has entered a time of significant changes and massive innovations. Traditional synchronous generators are being replaced by Renewable Energy Sources (RESs) that offer little or no inertia to the system as most of these energy sources are connected to the system via Power Electronic (PE) interfaces. Increasing penetration of PE-interfaced RESs will cause the total system inertia to dramatically decrease in the future [1]. In some countries, the power system's inertia has already reduced to certain levels endangering system stability and causing security challenges, a recent example of which is the power cut in the U.K. in August 2019 [2]. The integration of large intermittent RESs such as wind and solar power farms also results in the variation of system inertia as synchronous generators need to compensate for the power deficit when RESs are not committed to the system [3].

In order to arrest frequency deviations caused by large Loss of Generation (LoG) events, modern power systems resort to the disconnection of an appropriate amount of load, which is commonly known as Under Frequency Load Shedding (UFLS) [4]. Existing UFLS schemes can be categorized into three groups: traditional UFLS, semi-adaptive UFLS and adaptive UFLS [5]. Traditional UFLS schemes have several predefined steps, each of which is set to shed a certain amount of load once the corresponding frequency threshold is violated. Settings of traditional schemes are determined based on various presumed system parameters including system inertia [6], [7]. However, system conditions when the UFLS scheme is triggered are very often different than the presumed condition considered when setting the scheme. This may easily lead to significant over- or under-shedding [5], [8]. The predefined settings cannot provide adequate performance when the system inertia experiences large variations [9]–[11]. In order to overcome this problem, a great volume of research has been devoted to developing more adaptive UFLS solutions [12]–[17]. In semi-adaptive UFLS schemes, not only the frequency deviation but also the rate of change of frequency (RoCoF) at the relay location is considered to determine the timing and size of load shedding [4], [12]. Nonetheless, these methods are prone to shedding inappropriate amounts of load because the frequency and RoCoF measured at a certain location cannot fully represent the overall system frequency response, especially immediately after a LoG event [18].

With the advent of Wide Area Monitoring Systems (WAMSs), it has become possible to obtain the center of inertia (CoI) frequency to provide a holistic picture of the system frequency response for estimating the LoG event size by the swing equation [4]. This idea prompts several adaptive UFLS schemes, which are capable of adjusting the load shedding amount according to the estimated event size [13]–[17]. The scheme proposed in [13] is the first of its kind and takes a simple approach by shedding the same amount of load as the estimated event size in even steps. Adaptively setting the size of each UFLS step is proposed in [14] to lower the total amount of load shed by considering the

Mingyu Sun and Gaoyuan Liu are with the School of Electrical and Electronic Engineering, University of Manchester, Manchester M13 9PL, U.K. (e-mail: mingyu.sun@manchester.ac.uk; gaoyuan.liu@manchester.ac.uk).

Marjan Popov is with the Faculty of Electrical Engineering, Mathematics and Computer Science, Delft University of Technology, Delft 2628CD, the Netherlands (e-mail: m.popov@tudelft.nl).

Vladimir Terzija is with the Center for Energy Science and Technology, Skolkovo Institute of Science and Technology, Moscow 121205, Russia (e-mail: v.terzija@skoltech.ru).

Sadegh Azizi is with the School of Electronic and Electrical Engineering, University of Leeds, Leeds LS2 9JT, U.K. (e-mail: s.azizi@leeds.ac.uk).

system's primary frequency control. To achieve the same goal, the scheme proposed in [15] adjusts the load shedding amount according to a frequency stability boundary curve within the frequency-RoCoF plane. In [16], the allocation of load shedding to each load bus is optimized with respect to the bus voltage dip to improve the system voltage stability. Minimal load shedding is achieved in [17] by considering the ramp rate and rating of all generators. Despite their enhanced performance, these schemes pose demanding infrastructure requirements, such as Phasor Measurement Units (PMUs) at all generator terminals and reliable real-time communication networks between the control center and every UFLS relay. In fact, having such infrastructure already suffices to directly determine the LoG event size as all generators are monitored by PMUs. In addition, the centralized design of these schemes renders them vulnerable to communication failure and/or latency, which is the least wanted for a critically important system integrity protection scheme.

In this paper, a novel approach is used for estimating the CoI RoCoF using local measurements. To this end, an innovative technique referred to as Inflection Point Detector (IPD) is deployed. An inflection point is a point on the measured frequency curve at which the second derivative of frequency with respect to time crosses zero. By connecting the inflection points of the local frequency curve, the inter-area oscillations of frequency can be eliminated. With two consecutive inflection points, an approximate CoI RoCoF can be obtained. Then, an effective UFLS scheme is proposed to take advantage of the IPD technique for estimating the size of LoG using local information only. The inputs to the proposed scheme are the locally measured frequency and the total system inertia. The latter can be estimated in the control center using effective methods proposed in the literature such as [19]–[21] and transmitted to local relays on a minute-by-minute basis. The timescale is deemed sufficient as the system inertia may change when large synchronous generators are connected/disconnected to the grid, which may happen a few times a day. The proposed UFLS relay determines the LoG size and the amount of load to be shed based on the locally measured frequency and the most recent system inertia provided to it.

The rest of this paper is organized as follows. In Section II, the principles and challenges of calculating the CoI frequency and LoG size estimation are presented. Section III details the proposed IPD technique and proposed UFLS scheme. Section IV is devoted to performance evaluation by Real Time Digital Simulator (RTDS). Finally, section V concludes the paper.

II. PRINCIPLES AND CHALLENGES OF APPLYING THE SWING EQUATION FOR LoG EVENT SIZE ESTIMATION

Knowing the size of LoG events would be quite advantageous to improving approaches deployed for maintaining system stability. This can enable UFLS relays to swiftly shed an appropriate amount of load in order to retain active power balance. In this context, obtaining an approximate estimate of the LoG event size immediately after its inception would be more helpful than an accurate estimation of the LoG size after an unacceptably long delay. The sooner this size is estimated, the sooner an appropriate

amount of load can be shed from the power system to arrest frequency deviations.

The per-unit swing equation of a synchronous generator on its own apparent power base is expressed as follows

$$2H_i \frac{df_i}{dt} + D_i \Delta f_i = \Delta P_i \tag{1}$$

where H_i, D_i and Δf_i denote the inertia time constant, damping, and frequency deviation of the rotor of the generator i, respectively. ΔP_i is the pu difference between the mechanical input and electrical output active power of the generator i on the generator base. To come up with a single swing equation describing the overall system dynamics of a system with N synchronous generators, the CoI frequency is defined as

$$f_{CoI} = \sum_{i=1}^{N} H_i S_i f_i \Big/ \sum_{i=1}^{N} H_i S_i \tag{2}$$

where S_i denotes the rated power of generator i.

To apply the swing equation on a system with multiple generators, with some mathematical manipulations [1], [13], one can derive the following swing equation:

$$2H_{CoI} \frac{df_{CoI}}{dt} + D_{CoI} \Delta f_{CoI} = \Delta P_{CoI} \tag{3}$$

where

$$H_{CoI} = \frac{\sum_{i=1}^{N} H_i S_i}{\sum_{i=1}^{N} S_i}, \quad D_{CoI} = \frac{\sum_{i=1}^{N} D_i S_i}{\sum_{i=1}^{N} S_i},$$

$$\Delta P_{CoI} = \frac{\sum_{i=1}^{N} \Delta P_i S_i}{\sum_{i=1}^{N} S_i}$$

Equation (3) is commonly referred to as the CoI swing equation in per-unit. As we are mostly interested in the early periods following a LoG event in which frequency deviation term, i.e., $D_{CoI} \Delta f_{CoI}$, is much smaller than the other term on the left side of the equation, this term can be neglected [5]. Accordingly, (3) can be simplified to

$$2H_{CoI} \frac{df_{CoI}}{dt} = \Delta P_{CoI} \tag{4}$$

This equation relates the active power deficit to the CoI RoCoF, shortly after the LoG event inception.

CoI frequency is essentially defined as a weighted average of the rotor speeds of generators, not frequencies measured at generator terminals. To accurately estimate the CoI frequency, the internal voltage of each generator should be calculated. This may not be straightforward and introduces some errors due to the inaccuracy of generator parameters and their time-dependence. Alternatively, special metering equipment might be installed at each generator to directly measure its rotor speed, which might be demanding. Therefore, system operators may prefer to measure the frequency at some pilot buses in the system, instead of estimating the CoI frequency [22], [23]. Nonetheless, the frequency response of a pilot bus cannot accurately represent the weighted average frequency of the whole system, but only the average frequency of synchronous machines in its near vicinity.

The CoI swing equation can be used to estimate the size of a LoG event. This can form a UFLS scheme followed by sending

trip signals to some load blocks to compensate for the active power deficit in the system. Practically speaking, there are two main challenges to adopt such a communication-based UFLS scheme. Firstly, if all generator terminals are equipped with PMUs, the tripped generators and the resulting active power deficit can be directly determined without resorting to the CoI frequency. Secondly, designing the system stability countermeasures fully reliant on the communication network is not deemed quite prudent as the system-wide communication is prone to latency, corrupted data, or even total failure. It follows that an UFLS scheme based only upon such an approach may fail to determine the event size, and thus, to operate in a timely manner.

III. LOCAL ESTIMATION OF THE CoI RoCoF AND THE LoG EVENT SIZE

Considering the technical challenges described in the previous section, the real-time calculation of the CoI frequency using communication infrastructure might not be a viable option. Here, a simple yet effective technique is presented for estimating the CoI RoCoF using only locally measured frequency and not mandating PMUs at all generator terminals. The availability of the CoI RoCoF makes it possible to develop an adaptive UFLS scheme for power systems with volatile inertia. This can effectively prevent frequency from declining to unacceptably low nadirs following large LoG events.

A. Local Estimation of the CoI RoCoF

Following a LoG event in the system, frequencies at different locations of the system start declining. Frequency deviations will not be uniform across the system, despite demonstrating a relatively similar trend and eventually converging to the same value after several seconds. Following a LoG event, frequencies at different locations oscillate around the CoI frequency, and the differences between them vanish exponentially over time.

Simulations show that when the second derivative of the frequency with respect to time is positive, i.e., the frequency curve showing upward concaveness, its magnitude is smaller than the CoI frequency. On the contrary, when the second derivative of frequency with respect to time is negative, i.e., the frequency curve showing downward concaveness, its magnitude becomes larger than the CoI frequency. Between the upward and downward concaved sections lie inflection points where the second derivative of frequency with respect to time changes its sign. This forms the basis for the Inflection Point Detector (IPD), which is used in this paper to pinpoint inflection points in real-time. The local frequency curve intersects the CoI frequency curve at around the inflection points of the former. An approximate estimate of the CoI frequency can be obtained by connecting these inflection points, so that the CoI RoCoF can be obtained, accordingly. A mathematical proof of the theory in a two-bus system is provided in [24].

To demonstrate the principles of the proposed IPD, a LoG event is simulated on the IEEE 39-bus test system, and results are shown in Fig. 1. Fig. 1(a) demonstrates the calculated CoI frequency for an arbitrarily selected local frequency oscillating around the CoI frequency. The RoCoF of the local frequency,
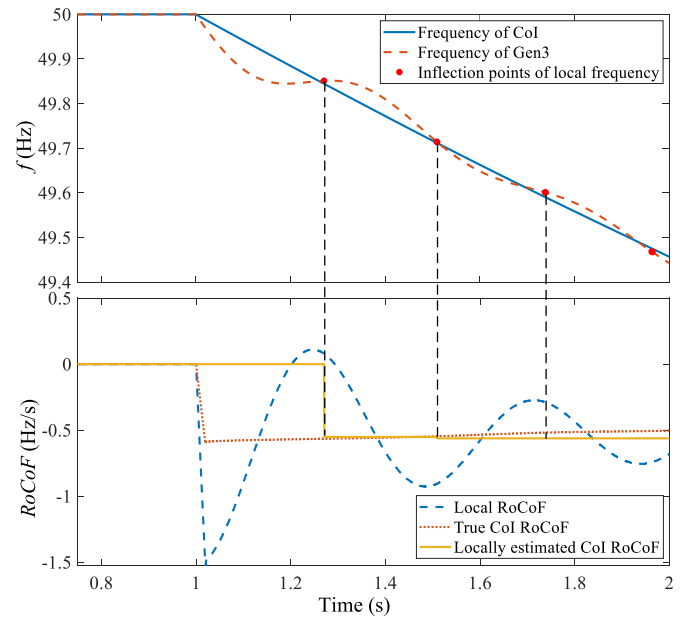

Fig. 1.   Local estimation of CoI RoCoF using the proposed IPD technique.
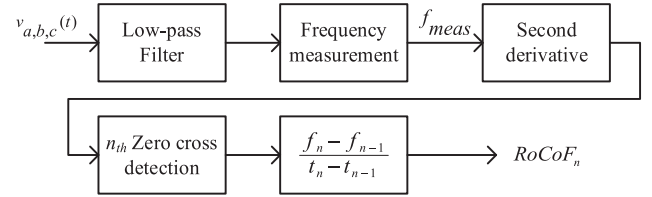

Fig. 2.   Block diagram of the Inflection Point Detector.

the CoI RoCoF and the one estimated by using the proposed IPD technique are shown in Fig. 1(b). This estimation is considered as a good approximation of the CoI RoCoF after the first inflection point is detected. The local frequency curve intersects with the CoI frequency curve when the second derivative of the former becomes zero. A rigorous mathematical proof of the theory for a two-source system can also be found in [24]. Let f_n and t_n denote the frequency and time instant of the n-th inflection point on the local frequency curve. Besides, f_0 and t_0 refer to the coordinates of the LoG inception instant on the frequency curve. The IPD estimates the CoI RoCoF as follows

$$\frac{df_{CoI}}{dt} \Big|_{t=\frac{t_n-t_{n-1}}{2}} \approx \frac{f_n - f_{n-1}}{t_n - t_{n-1}} \tag{5}$$

Fig. 2 shows the block diagram of the IPD used for estimating the CoI RoCoF using local frequency measurements.[1]

B. Proposed UFLS Scheme

Having estimated the CoI RoCoF as described, the LoG event size can be calculated using the swing equation assuming that the

---

[1]This is the simplest way to calculate first derivative. Other approaches, more immune to random noise existing in the processed frequency signal, but involving more samples could be used, if needed [21].

system inertia is known. The question arising here is whether it is possible to conduct UFLS using just local information without communication between the control center and UFLS relays. Using such a *non-communication approach* must ensure that the total load shed by different relays is equal to the active power deficit in the system. Let us assume that N substations are equipped with the proposed UFLS relays. Let m_i^f denote the locally estimated CoI RoCoF at the location i. Besides, m_i^f is assumed to be the slope of the straight line between the point on the frequency curve at $t = 0^-$ and the first inflection point detected on this curve. With the assumption that locally estimated CoI RoCoFs are an adequate approximation of the true CoI RoCoF, one can obtain

$$m_1^f \cong m_2^f \cong \cdots \cong m_N^f \cong m_{CoI}^f \cong \frac{\Delta f_{CoI}}{\Delta t} \quad (6)$$

where the true RoCoF refers to the average RoCoF of the CoI on the interval from the event inception to the instant of the first inflection point on the local frequency curve. Let us assume that the system inertia is regularly, e.g., every minute, updated in the UFLS relays. Thus, each relay can individually estimate the size of the active power deficit in MW from

$$\Delta P_i^{est} = 2H_{CoI}S_{CoI}m_i^f \quad (7)$$

where S_{CoI} refers to the total power capacity of synchronous generators. The superscript "*est*" in ΔP_i^{est} implies that this variable is the estimation of the LoG size by the relay at the location i. The amount of load to be shed by the relay i is denoted by δP_i and is calculated as

$$\delta P_i = \underbrace{2H_{CoI}S_{CoI}m_i^f}_{\Delta P_i^{est}} \frac{P_{L,i}}{\Delta P_{\text{total}}} \quad (8)$$

where $P_{L,i}$ is the maximum amount of load allocated for load shedding at the location i and ΔP_{total} is the size of the largest credible contingency in the system. It can be easily confirmed that the sum of δP_i at all UFLS-enabled locations will be equal to the LoG size provided that

$$\sum_{i=1}^{n} P_{L,i} = \Delta P_{total} \quad (9)$$

It should be noted that due to the governor response of synchronous generators and the frequency dependency of load, it is not necessary to shed the exact amount of load as the LoG event size to retain a balance between generation and consumption [25]. This can be considered by applying an adjustment coefficient β to the estimated LoG size by (7). Then (8) can be rewritten as

$$\delta P_i = 2\beta H_{CoI}S_{CoI}m_i^f \frac{P_{L,i}}{\Delta P_{total}} \quad (10)$$

This yields the amount of load that needs to be shed at the location i in the system. The flowchart of the proposed UFLS scheme is shown in Fig. 3. Each UFLS relay detects the occurrence of LoG events when the locally measured $RoCoF_i$ exceeds the threshold (0.1 Hz/s in this study). Following the event detection, a blocking period of T_{D1} (500 ms in this study) is applied before seeking the first inflection point using the IPD.
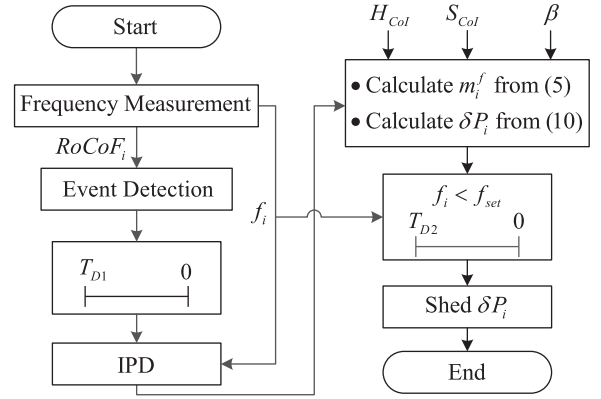

Fig. 3. Flowchart of the proposed UFLS scheme.

This is to avoid identifying false inflection points within the transient period following the LoG event. The required load shedding amount δP_i is determined from (10). Load shedding is not initiated unless the frequency threshold f_{set} (49.5 Hz in this study) is violated for an intentional time delay of T_{D2} (150 ms in this study). This time delay is to provide sufficient time for all relays to make a proper decision before any load shedding starts in the system. This is to further add to the security of the method as inflection points are usually identified well before the frequency threshold being triggered. This means relays already know how much load to shed and the initiation of load shedding elsewhere will not affect any relay's ability to determine the disturbance size and the amount of load to shed.

It is assumed in (7) that the system inertia remains unchanged after the LoG event. This assumption holds if the LoG event is caused by the disconnection of HVDC inter-connectors or PE-interfaced RESs with negligible inertia contribution. However, if the LoG is caused by the trip of a synchronous generator, relying on the constant inertia assumption would lead to the overestimation of the LoG size [26]. Therefore, an inertia compensation technique is proposed here to offset the effect of system inertia reduction due to the tripped generator on the LoG size estimation. To account for this and make the estimation more accurate, (7) can be rewritten as

$$\Delta P_i^{est} = 2H_{post}S_{post}m_i^f \quad (11)$$

where H_{post} and S_{post} denote the aggregate system inertia and power capacity following the LoG event, respectively. Therefore, the relationship between the pre-event and post-event kinetic energy of rotating masses in the system with that of the tripped generator can be written as follows

$$2H_{CoI}S_{CoI} = 2H_{post}S_{post} + 2H_tS_t \quad (12)$$

where H_t and S_t refer to the inertia constant and power capacity of the tripped generator, respectively. One can use

$$S_t = P_t/PF \quad (13)$$

to calculate the power capacity of the tripped generator where P_t and PF are the active power output and power factor of the
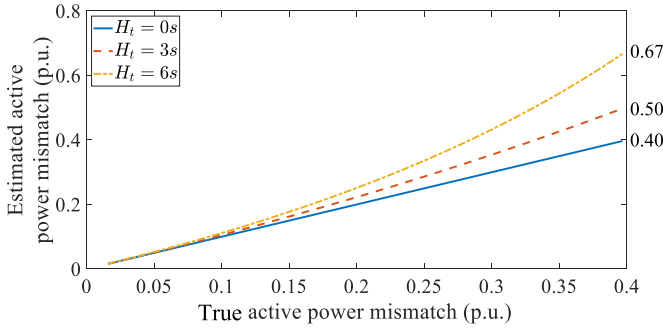
Fig. 4.   Estimated LoG size for LoG events with different inertia.

Fig. 5.   Single-line diagram of the IEEE 39-bus test system.

tripped generator, respectively. Substituting (13) into (12) yields

$$2H_{CoI}S_{CoI} = 2H_{post}S_{post} + 2H_t P_t / PF \qquad (14)$$

The value of P_t can be estimated by (11). Substituting the term on the right-hand side of (11) into (14) gives

$$H_{CoI}S_{CoI} = H_{post}S_{post} - 2H_t H_{post}S_{post}m_i^f / PF \qquad (15)$$

Rearranging (15) in terms of $H_{post}S_{post}$ and substituting it into (11) gives a more accurate estimate of the LoG size as below

$$\Delta P_i^{est} = \frac{2H_{CoI}S_{CoI}}{1 - 2H_t m_i^f / PF} m_i^f \qquad (16)$$

Note that in the case of a LoG event without inertia contribution, applying the proposed inertia compensation would result in an underestimation of the LoG size. However, the advantage of applying the above inertia compensation outweighs this disadvantage as overshedding by the UFLS relays can be avoided in this way. A detailed sensitivity analysis is carried out to study the impact of inertia constant and size of the tripped generator on the accuracy of the swing equation-based LoG size estimation. Fig. 4 shows the estimation error when the proposed inertia compensation technique is not applied. Here, the inertia constant of the tripped generator H_t is varied between 0 and 6 sec, and the LoG size is set to 0.4 pu.

It can be seen that the larger the inertia of the tripped generator is, the bigger the LoG estimation error becomes for the same LoG size. If the LoG size is relatively small compared to the total generation in the system, the effect can be neglected. The estimation error increases as the disturbance size increases. The error of the estimated LoG size reaches 68.75% when the disturbance size is 40% of the total system generation, and the inertia constant of the tripped generator is 6 sec. The power factor used in this technique can be obtained as a weighted average power factor of all generators based on historical data. In all simulations carried out in the next section, an average inertia of 3 sec and a weighted average power factor of all generators are assumed for the lost generation. This is to make a tradeoff between over- and under-estimation of the LoG size.

IV. PERFORMANCE EVALUATION

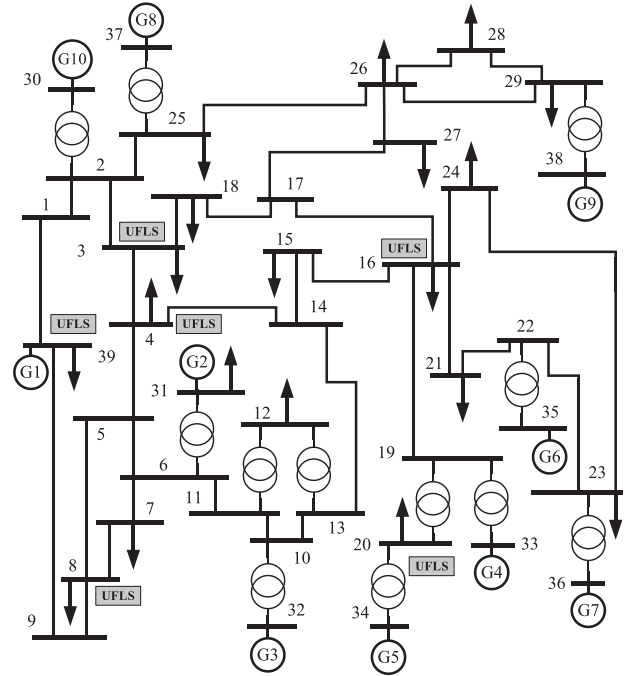In this section performance of the proposed UFLS scheme is studied. An extensive number of simulations are carried out

on the IEEE 39-bus test system [27]. The single-line diagram of this test system is provided in Fig. 5. Real Time Digital Simulator (RTDS) is used to conduct simulation studies. The test system is modeled in RSCAD software and loaded to one RTDS rack, which runs in real-time with a 65-μs time-step. The UFLS relays are modeled using RSCAD and loaded to another RTDS rack. Both racks are connected to each other with internal communication links, providing the relays with local three-phase voltage waveforms, and linking their trip commands to corresponding load blocks in the test system. All results reported in the paper are obtained with a sampling rate of 1.6 kHz for the local three-phase voltage in order to estimate frequency with a reporting rate of 50 Hz by the Discrete Fourier Transform (DFT). The cut-off frequency of the low-pass filter in the IPD is set to 100 Hz. The time-step used for computing the second derivative of the measured frequency is 1 cycle.

Each synchronous generator in the system is equipped with the IEEE type 1 excitation system and TGOV1 governor model. The ZIP load model with 20% constant impedance, 40% constant current and 40% constant power is used for loads in the study. RES generators are each modelled as a dynamic PQ source with phase locked loop and current control [28] and placed at every generator terminal to uniformly replace different portions of synchronous generation, accounting for different levels of RES penetration. In this way, four operating scenarios with different inertia levels are considered. System frequency responses for different operating scenarios are obtained and analyzed. Results obtained are used to evaluate the effectiveness of the proposed UFLS scheme and to compare it with that of the conventional scheme. The CoI frequency is used as an indicator of the whole system's frequency behavior. The

Scenario	System Inertia		System Capacity
	MVA.s	Sec	(MVA)
Base Case	78000	12.4	6300
25% RES	58500	9.3	6300
50% RES	39000	6.2	6300
75% RES	19500	3.1	6300

focus of this paper is UFLS, whose role is to arrest substantial frequency deviations following a LoG event. Therefore, the final frequency after load shedding will be different than the nominal frequency, as this is the responsibility of the secondary frequency control.

A. Test System and UFLS Settings

The IEEE 39-bus test system with a total load capacity of 6087 MW and 2781 MVAr is used to test the performance of the proposed and conventional UFLS schemes in terms of system frequency response following different LoG events. The nominal frequency of this system, which is originally 60 Hz, is modified to be 50 Hz. RESs are added to all generator buses. The RES penetration level is varied by replacing different portions of conventional generation by equivalent renewable generation. To create under frequency conditions, generators of different sizes at different locations are tripped. Four versions of the IEEE 39-bus test system in RTDS are created to represent the system in future scenarios with different inertia and RES penetration levels. Table I lists the information of each scenario in terms of system capacity and inertia. The test systems corresponding to these scenarios are called base-case, 25% RES case, 50% RES case and 75% RES case, respectively. The base-case scenario represents the default scenario with the largest inertia of 12.4 sec. The UFLS relays are placed at one-third of the load buses. It is noted that the location of relays is not the major concern of this study as it is a common practice to assume all relays and generators are connected to a single bus when studying the UFLS performance in terms of the frequency nadir and post-event steady state frequency.

The proposed UFLS relays are set to operate and shed an appropriate amount of load once the local frequency falls below 49.5 Hz. For comparison, a five-step conventional UFLS scheme is implemented, which disconnects a total of 400 MW load upon the violation of each of the 49.5, 49.2, 49.0, 48.8 and 48.6 Hz frequency thresholds. A 150 ms delay is added to represent the operation delay of circuit breaker. This enables us to compare the performances of the proposed and conventional UFLS schemes following similar LoG events. The settings of the conventional scheme are obtained based on relevant grid code guidelines and common practice [10], [12]. System inertia is assumed to be estimated with respect to the committed synchronous generators in the system and fed to the UFLS relays regularly enough via non-real-time communication media. The scheme successfully counteracts the active power deficit through this single step of load shedding.
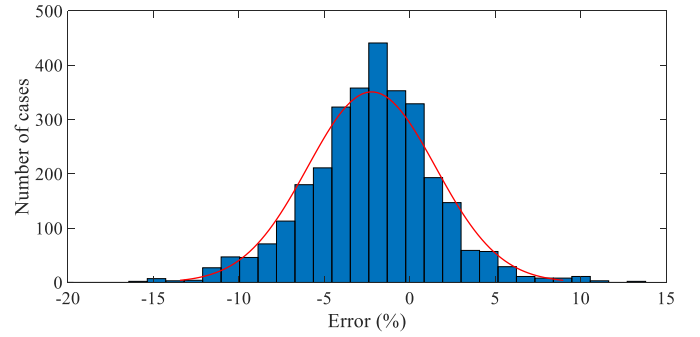

Fig. 6.   The distribution of the RoCoF estimation error.

B. Accuracy of the Local RoCoF Estimation

To study the accuracy of the proposed local CoI RoCoF estimation technique and the impact of the relay location on the method, all 29 non-generator buses are equipped with the proposed UFLS relays. A total of 105 LoG events are simulated at different locations with sizes ranging from 250 MW to 1250 MW in 50 MW steps. In total, 3045 RoCoF estimations are acquired and presented in Fig. 6. About 88.2% of all local CoI RoCoF estimations are within 5% deviation of the true CoI RoCoF, which shows great accuracy and robustness of the proposed IPD technique. It should be also noted that the mean and standard deviation of RoCoF estimation errors are -2.23% and is 3.73%, respectively.

Let us assume the CoI RoCoF estimation error has normal distribution with mean μ and standard deviation δ. Based on the 3δ criterion, the local CoI RoCoF estimation error will lie within the range $\mu \pm 3\delta$ with a confidence level of 99.7%. Let us also suppose that there are k UFLS relays in the system, each of which is set to shed $1/k$ of its estimated LoG size. Therefore, the total LoG size estimation error based on proposed method will be limited to the range $\mu \pm 3\delta/\sqrt{k}$. For a k of 6, this means the overall error of LoG size estimation would lie between -6.80% to $+2.34\%$ of the real LoG size, which agrees with extensive simulations conducted.

C. General Evaluation of the Proposed UFLS Scheme

The performance of the proposed UFLS scheme is studied in this subsection for a wide range of LoG events in different system scenarios. A heavy loading scenario is created with a 1500 MW load and generation increase. The outage of generating units below 600 MW will not activate the UFLS scheme as frequency deviation will not violate the 49.5 Hz threshold. Four larger outage cases of 600, 800, 1000 and 1200 MW makes frequency violate the 49.5 Hz frequency threshold. To demonstrate the performance of the UFLS scheme following these four LoG events, the CoI frequency following each event is calculated using (2) and shown in Fig. 7. It is obvious that the UFLS scheme successfully arrests frequency deviations in all cases. The first inflection point is detected in all cases around 600 ms after the LoG event. The frequency nadir remains quite close to 49.5 Hz regardless of the event size. This is because the whole generation
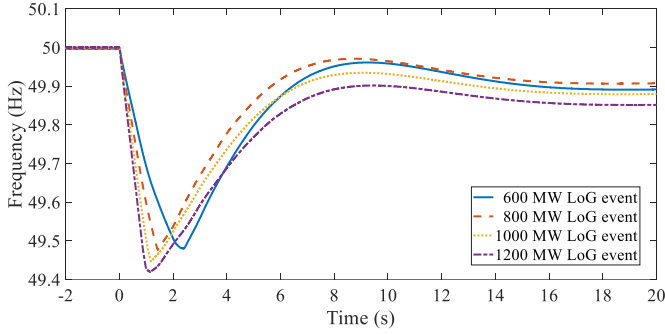
Fig. 7. The frequency response of the proposed UFLS scheme following LoG events of different size.

Fig. 8. The frequency response of the proposed and conventional UFLS schemes for different RES penetration levels.

TABLE II
PERFORMANCE OF THE PROPOSED UFLS SCHEME

LoG Size (MW)		Load Shed (MW)	RoCoF (Hz/s)		RoCoF Est. Error (%)
True	Estimated		True	Estimated	
600	498.8	416.5	-0.316	-0.319	0.97%
800	644.5	642.2	-0.415	-0.412	-0.72%
1000	790.4	787.7	-0.512	-0.505	-1.39%
1200	936.2	933.0	-0.604	-0.598	-1.02%

TABLE III
UFLS TRIGGERING INSTANTS BY DIFFERENT RELAYS

LoG Size	600 MW	800 MW	1000 MW	1200 MW
Relay 1	2.36 s	1.38 s	1.14 s	0.95 s
Relay 2	2.37 s	1.38 s	1.13 s	0.95 s
Relay 3	2.23 s	1.38 s	1.13 s	0.94 s
Relay 4	2.38 s	1.39 s	1.14 s	0.97 s
Relay 5	--- s	1.38 s	1.15 s	1.09 s
Relay 6	2.05 s	1.40 s	1.02 s	0.84 s

imbalance is compensated immediately after the threshold has been violated.

The average RoCoF estimation error is calculated as

$$\text{Average Relative Error} = \frac{1}{N} \sum_{i=1}^{N} \left| \frac{RoCoF_{CoI} - m_i^f}{RoCoF_{CoI}} \right| \quad (17)$$

where the $RoCoF_{CoI}$ stands for the true CoI RoCoF, and m_i^f and N are the estimated RoCoF by the relay i and the number of UFLS relays in the system, respectively.

Table II summarizes the true and estimated LoG size and CoI RoCoF in each simulated case. As can be seen, the estimations are quite acceptable from a practical point of view, with marginal errors. The estimation error for CoI RoCoF in all cases are less than 2%. Furthermore, the estimated LoG size is smaller than the true size. This discrepancy is related to the inertial response of generators and the effect of voltage depression immediately after the event [23]. Table III shows the time instants at which the UFLS relays disconnect their corresponding load blocks. In the case of 600 MW LoG, one relay is not triggered as the load shed by other relays is enough to make frequency recover.
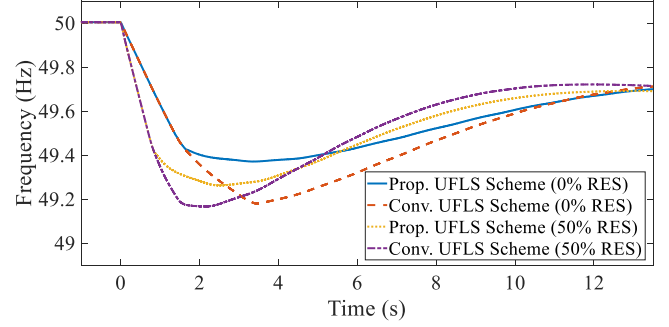
TABLE IV
AVERAGE RoCoF ESTIMATION ERROR BY THE PROPOSED UFLS SCHEME FOR DIFFERENT RES PENETRATION LEVELS

LoG Event Size (MW)	Base case	25% RES	50% RES	75% RES
1000	2.66%	3.25%	6.53%	6.09%
1200	2.05%	4.79%	7.00%	8.20%
1400	2.40%	3.39%	6.18%	8.43%
1600	1.50%	4.18%	4.14%	6.59%
1800	0.21%	3.73%	3.96%	7.27%

D. Sensitivity to Various Factors

The UFLS sensitivity to RES penetration level is investigated in this subsection by comparing the performances of the proposed and conventional UFLS schemes. A wide range of event sizes is considered by disconnecting 5% to 25% of the total generation in the system. For each specific event size, multiple possible cases are studied to ensure obtained results and conclusions drawn are valid.

Fig. 8 demonstrates the frequency response following a 1400-MW LoG event with 0% and 50% RES penetration level respectively. The adjustment coefficient β is set to 0.7 pu for the proposed scheme to have a similar amount of load shedding as the conventional scheme. This aspect will be further detailed in Subsection IV-F. The solid and dashed lines represent results obtained by the proposed and the conventional UFLS scheme, respectively. As can be seen, the proposed UFLS scheme arrests frequency deviations more effectively and contains the frequency nadir close to the nominal frequency thanks to its ability to estimate the true LoG size fast and accurately. Table IV summarizes the results of RoCoF estimation for different RES penetration levels. The average relative error does not exceed 9% in any of penetration levels studied, confirming that the accuracy of the proposed technique is quite promising from a practical point of view. This confirms that the proposed method performs well in defending the system against LoG events when RES penetration level varies.

Table V provides frequency nadirs for LoG events of sizes ranging from 1000 MW to 1800 MW, with increments of 200 MW. As can be seen, the nadir by the proposed scheme does not fall as much as that by the conventional UFLS scheme irrespective of the RES penetration level. This is because of

TABLE V
FREQUENCY NADIRS FOR DIFFERENT RES PENETRATION LEVELS

LoG Event Size (MW)	Base-Case		25% RES		50% RES		75% RES	
	Prop.	Conv.	Prop.	Conv.	Prop.	Conv.	Prop.	Conv.
	Frequency Nadir (Hz)							
1000	49.48	49.40	49.46	49.37	49.45	49.32	49.40	49.23
1200	49.46	49.25	49.44	49.20	49.42	49.18	49.34	49.18
1400	49.43	49.18	49.42	49.18	49.40	49.17	49.36	49.09
1600	49.42	49.15	49.41	49.14	49.36	49.02	49.33	49.00
1800	49.39	49.00	49.37	49.00	49.31	48.98	49.20	48.89

the fast estimation of the event size and implementation of the UFLS instantaneously by the former. On the other hand, the amounts of load shed by the proposed UFLS scheme remain constant regardless of the RES penetration level and the system inertia. However, simulation results show that the conventional UFLS scheme tends to shed more load following a LoG event of a fixed size if the system inertia decreases. This emanates from the fixed margins between the frequency thresholds of the conventional UFLS scheme. Indeed, for larger RES penetration levels, frequency drops much faster and is likely to violate a greater number of frequency thresholds before the load shedding steps take effect. This will result in more load shedding and even overshedding in systems with highly reduced inertia.

E. Comparison With the Centralized UFLS Scheme

To demonstrate how the proposed local UFLS scheme could outperform communication-based UFLS schemes, the ideal centralized UFLS scheme proposed in [13] is considered here. In the centralized scheme, it is assumed that the CoI RoCoF can be accurately calculated using PMU data in order to estimate the active power deficit by the swing equation. Load shedding is applied proportionally across the system in one step. The latency of the centralized scheme is assumed to have a normal distribution with 300 ms mean and 100 ms standard deviation including communication latency and circuit breaker operation time [29]. The latency of the proposed scheme is attributed to the circuit breaker operation time which is considered to have a mean of 150 ms and a standard deviation of 40 ms. The performances of these UFLS schemes are compared in terms of frequency nadir and the time each scheme takes to initiate the UFLS process following the same LoG event.

A total of 10000 cases of 1000 MW LoG events are simulated with 50% RES penetration level. Fig. 9 demonstrates the time distribution of the implementation of the load shedding process by the proposed and the centralized UFLS schemes. The term "*time to initiate load shedding*" is defined as the time passed after the 500 ms blocking period. As can be seen, the proposed scheme initiates the UFLS process, on average, 150 ms earlier than the centralized scheme. On the other hand, the time distribution of UFLS initiation by the centralized scheme spans over a larger range. UFLS initiation time will directly impact the frequency nadir reached by each of the UFLS schemes, as shown in Fig. 10.
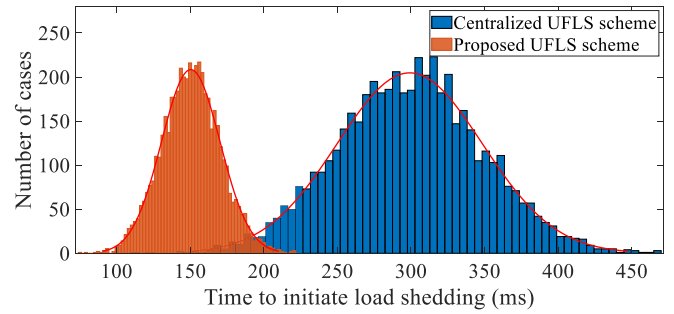

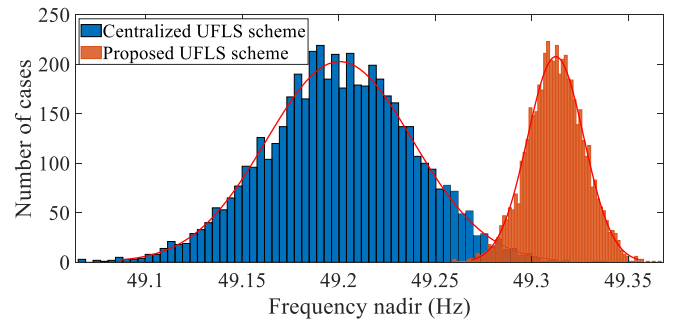Fig. 9. Time distribution of initiating the UFLS process by the proposed and centralized UFLS schemes.

Fig. 10. Frequency nadirs reached by the proposed and centralized UFLS schemes.

Although both schemes successfully contain frequency deviations, the nadir by the proposed scheme lies on average 0.1 Hz above that by the centralized scheme. This demonstrates an extra advantage that can be gained by not resorting to communication for UFLS in the power system.

F. An Adjustment Coefficient to Optimize UFLS Performance

The flexibility offered by the fast estimation of the LoG size using the proposed UFLS scheme is demonstrated in this subsection. The amount of load shed by the conventional UFLS scheme is generally smaller than the LoG size. This essentially results from the multiple load shedding steps used by the conventional UFLS scheme. If frequency violates a frequency threshold but does not reach the next threshold, only the amount attributed to the violated threshold will be shed from the system. However, the proposed scheme is able to accurately estimate the size of the LoG event. This enables system operators to decide what portion of the lost active power needs to be compensated for by load shedding.

In practice, it might be desirable to limit the load shedding amount to a less-than-unity fraction of the LoG size. Many studies on adaptive UFLS, e.g., [15] and [16], have also deliberately reduced a certain portion of the estimated power deficit to shed less amount of load. This can be done in the proposed scheme simply by multiplying the estimated LoG size by an adjustment coefficient. Special care should be taken to determine the adjustment coefficient since shedding less amount of load
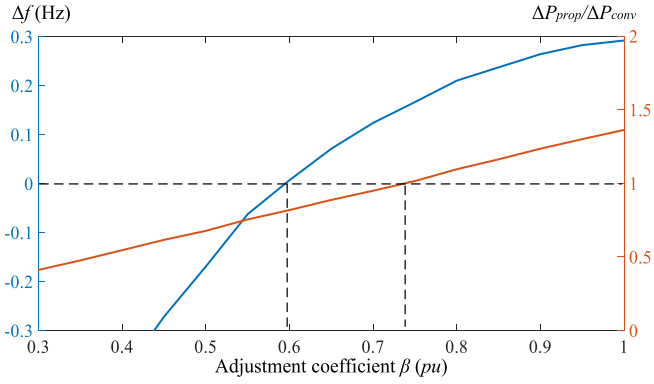
Fig. 11. Performance optimization of the proposed UFLS scheme by varying the adjustment coefficient.

Fig. 12. CoI frequency response using different adjustment coefficients.

will certainly result in lower frequency nadir and final system frequency.

The performances of the proposed UFLS scheme with different adjustment coefficients, and the conventional UFLS scheme are compared here. This comparison is undertaken in terms of the frequency nadir reached and the total amount of load shed. To this end, the IEEE 39-bus test system with 50% RES penetration is used. The sizes of LoG events are varied from 1200 MW to 1800 MW, and the frequency behavior is recorded for adjustment coefficients ranging from 0 to 1 pu. Fig. 11 summarizes important behavioral indices of results obtained. In this figure, ΔP_{prop} and ΔP_{conv} refer to the total amount of load shed by the proposed and conventional UFLS schemes, respectively. It can be seen that with no adjustment ($\beta = 1$) the frequency nadir obtained by the proposed scheme will be located 0.3 Hz higher than that with the conventional scheme. This is achieved by shedding the same amount of load as the LoG event size.

By decreasing the adjustment coefficient, the amount of load shed by the proposed scheme will decrease at the expense of reaching lower nadirs. For $\beta = 0.74$, the amount of load shed by the proposed scheme will be fairly equal to that by the conventional scheme, whilst ensuring a higher nadir. The reason is that the load shedding process by the proposed scheme is done once the frequency falls below 49.5 Hz, while this is done in several steps using the conventional scheme. Further reduction of β gives rise to higher frequency nadirs but with less amount of load shed by the proposed scheme compared to these by the conventional UFLS scheme. This superiority continues up until $\beta = 0.6$ for which the nadir with both schemes will be the same, while the amount of load shed by the proposed scheme is less than 50% of that by the conventional scheme. In practice, the performance of the proposed method may be further optimized using the adjustment coefficient β. This would require a set of offline simulation studies, as the optimal value of β might be slightly different for different networks.

Fig. 12 demonstrates the frequency response of the system for a 1400 MW LoG event using the proposed UFLS scheme and compares it with the one obtained by the conventional UFLS schem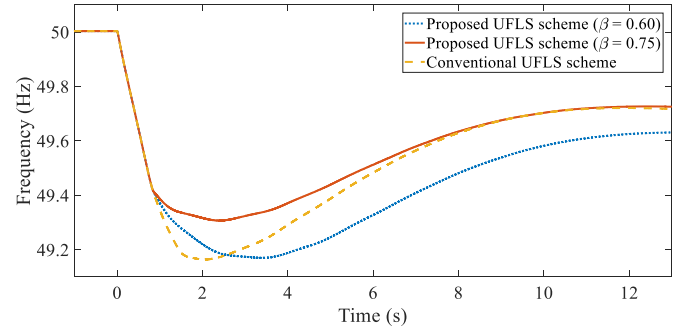e. When $\beta = 0.75$ pu, the proposed scheme will shed the same amount of load as that by the conventional scheme. In this case, the maximum frequency deviation is 0.15 Hz less than that by the conventional UFLS scheme. Fig. 11 also shows how the same nadir would be achieved by the proposed scheme by setting $\beta = 0.6$ pu only by shedding 80% of the load shed by the conventional scheme. In this case, the time needed to reach the nadir is increased, which gives the opportunity for primary and secondary control mechanisms to return the frequency within an acceptable range in due time. Therefore, the proposed scheme can provide higher frequency nadirs than that by the conventional UFLS scheme, with equal or even less amount of load shed.

V. CONCLUSION

Conventional UFLS schemes may not be able to contain frequency deviations in power systems with volatile inertia without introducing the risk of overshedding or reaching low frequency nadirs. An effective local UFLS scheme is proposed in this paper with no need of real-time communication. The proposed scheme uses local frequency measurements to estimate the RoCoF of the center of inertia. This helps to estimate the size of lost generation and adaptively change the amount of load to be shed. Simulation results confirm that the proposed scheme outperforms the conventional and centralized UFLS schemes in terms of containing frequency deviations. The load shedding is carried out in a single step when the frequency falls below a predetermined frequency threshold. Not relying on real-time communication infrastructure, the proposed scheme is able to provide a frequency nadir of around 49.3 Hz irrespective of the event size, RES penetration level, and thus system inertia. These features are beyond the capabilities of existing UFLS schemes. The simple logic of the proposed scheme can be easily integrated into modern intelligent electronic devices at substations. Having such an adaptive UFLS scheme will be quite beneficial to fortifying the last line of defense against frequency instability in future power systems with volatile inertia.
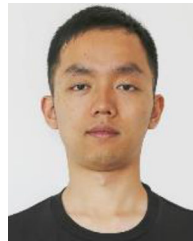
REFERENCES

[1] A. Ulbig, T. S. Borsche, and G. Andersson, "Impact of low rotational inertia on power system stability and operation," *IFAC Proc.*, vol. 19, pp. 7290–7297, 2014.

[2] National Grid ESO. "Technical report on the events of 9 august," 2019. [Online]. Available: https://www.nationalgrideso.com/document/152346/download

National Grid ESO. "Electricity ten year statement," 2018. [Online]. Available: https://www.nationalgrideso.com/document/133836/download

[4] P. Kundur, *Power System Stability And Control*. New York, NY, USA: McGraw-Hill, Inc, 1994.

[5] U. Rudez and R. Mihalic, "WAMS-based underfrequency load shedding with short-term frequency prediction," *IEEE Trans. Power Del.*, vol. 31, no. 4, pp. 1912–1920, Aug. 2016.

[6] H. E. Lokay and V. Burtnyk, "Application of underfrequency relays for automatic load shedding," *IEEE Trans. Power App. Syst.*, vol. PAS-87, no. 3, pp. 776–783, Mar. 1968.

[7] S. H. Horowitz and A. G. Phadke, *Power System Relaying*. Hoboken, NJ, USA: Wiley, 2008.

[8] L. Sigrist, I. Egido, and L. Rouco, "Performance analysis of UFLS schemes of small isolated power systems," *IEEE Trans. Power Syst.*, vol. 27, no. 3, pp. 1673–1680, Aug. 2012.

[9] National Grid ESO. "Low frequency demand disconnection," *Report*, 2017. [Online]. Available: https://www.nationalgrideso.com/document/87836/download

[10] Work Package 4. "D4.2 limitations of present AC protection schemes and SIPS technologies to properly operate in systems with high penetration of PE during faults in DC and AC systems," MIGRATE Project, 2017.

[11] P. He, B. Wen, and H. Wang, "Decentralized adaptive under frequency load shedding scheme based on load information," *IEEE Access*, vol. 7, pp. 52007–52014, 2019.

[12] D. Prasetijo, W. R. Lachs, and D. Sutanto, "A new load shedding scheme for limiting underfrequency," *IEEE Trans. Power Syst.*, vol. 9, no. 3, pp. 1371–1378, Aug. 1994.

[13] V. V. Terzija, "Adaptive underfrequency load shedding based on the magnitude of the disturbance estimation," *IEEE Trans. Power Syst.*, vol. 21, no. 3, pp. 1260–1266, Aug. 2006.

[14] U. Rudez and R. Mihalic, "Monitoring the first frequency derivative to improve adaptive underfrequency load-shedding schemes," *IEEE Trans. Power Syst.*, vol. 26, no. 2, pp. 839–846, May 2011.

[15] L. Sigrist, I. Egido, and L. Rouco, "Principles of a centralized UFLS scheme for small isolated power systems," *IEEE Trans. Power Syst.*, vol. 28, no. 2, pp. 1779–1786, May 2013.

[16] S. Abdelwahid, A. Babiker, A. Eltom, and G. Kobet, "Hardware implementation of an automatic adaptive centralized underfrequency load shedding scheme," *IEEE Trans. Power Del.*, vol. 29, no. 6, pp. 2664–2673, Dec. 2014.

[17] Y. Tofis, S. Timotheou, and E. Kyriakides, "Minimal load shedding using the swing equation," *IEEE Trans. Power Syst.*, vol. 32, no. 3, pp. 2466–2467, May 2017.

[18] F. Milano, "Rotor speed-free estimation of the frequency of the center of inertia," *IEEE Trans. Power Syst.*, vol. 33, no. 1, pp. 1153–1155, Jan. 2018.

[19] J. Zhao, Y. Tang, and V. Terzija, "Robust online estimation of power system center of inertia frequency," *IEEE Trans. Power Syst.*, vol. 34, no. 1, pp. 821–825, Jan. 2019.

[20] K. Tuttelberg, J. Kilter, D. Wilson, and K. Uhlen, "Estimation of power system inertia from ambient wide area measurements," *IEEE Trans. Power Syst.*, vol. 33, no. 6, pp. 7249–7257, Nov. 2018.

[21] M. Sun, Y. Feng, P. Wall, S. Azizi, J. Yu, and V. Terzija, "On-line power system inertia calculation using wide area measurements," *Int. J. Electr. Power Energy Syst.*, vol. 109, pp. 325–331, 2019.

[22] M. Dreidy, H. Mokhlis, and S. Mekhilef, "Inertia response and frequency control techniques for renewable energy sources: A review," *Renew. Sustain. Energy Rev.*, vol. 69, pp. 144–155, 2017, [Online]. Available: http://dx.doi.org/10.1016/j.rser.2016.11.170

[23] U. Rudez and R. Mihalic, "Analysis of underfrequency load shedding using a frequency gradient," *IEEE Trans. Power Del.*, vol. 26, no. 2, pp. 565–575, Apr. 2011.

[24] S. Azizi, M. Sun, G. Liu, and V. Terzija, "Local frequency-based estimation of the rate of change of frequency of the center of inertia," *IEEE Trans. Power Syst.*, vol. 35, no. 6, pp. 4948–4951, Nov. 2020.

[25] S. Azizi, M. Rezaei Jegarluei, A. S. Dobakhshari, G. Liu, and V. Terzija, "Wide-area identification of the size and location of loss of generation events by sparse PMUs," *IEEE Trans. Power Del.*, vol. 36, no. 4, pp. 2397–2407, Aug. 2021.

[26] R. Azizipanah-Abarghooee, M. Malekpour, M. Paolone, and V. Terzija, "A new approach to the on-line estimation of the loss of generation size in power systems," *IEEE Trans. Power Syst.*, vol. 34, no. 3, pp. 2103–2113, May 2019.

[27] T. Athay, R. Podmore, and S. Virmani, "A practical method for the direct analysis of transient stability," *IEEE Trans. Power App. Syst.*, vol. PAS-98, no. 2, pp. 573–584, Mar. 1979.

[28] RTDS technologies. *Dynamic PQ Source*. Winnipeg, MB, Canada: RTDS Technologies, 2018.

[29] M. Golshani, "Novel performance evaluation of information and communication technologies to enable wide area monitoring systems for enhanced transmission network operation," Ph.D. thesis, Brunel Univ. London, 2015.

Mingyu Sun (Member, IEEE) received the B.Eng. degree in electrical engineering from Shandong University, Jinan, China, in 2013, and the M.Sc. and Ph.D. degrees in electrical power engineering from The University of Manchester, Manchester, U.K., in 2014 and 2020, respectively. Since 2019, he has been an Associate Innovation Engineer with National Grid Electricity Transmission, U.K. His research interests include application of power electronics in power systems, and wide-area monitoring, protection, and control systems. He is a Member of Cigré and actively participated in WG B4.90.

Gaoyuan Liu (Student Member, IEEE) received the B.Eng. (Hons.) degree with top rank in electrical and electronic engineering from The University of Manchester, Manchester, U.K., and the B.Eng. degree in electrical engineering and its automation from North China Electric Power University, Beijing, China, in 2015. He is currently working toward the Ph.D. degree with The University of Manchester, Manchester, U.K. In November 2019, he was with the Institute of Communication and Power Networks, the University of Leeds, Leeds, U.K. as a Visiting Researcher. From March 2017 to January 2019, he worked on the protection Work Package of the EU H2020 MIGRATE project, and since January 2019, he was the Leader of the research team with the University of Manchester. His research interests include wide-area monitoring and protection, system integrity protection schemes, and large-scale integration of renewable energy sources.

Marjan Popov (Senior Member, IEEE)) received the Dipl.-Ing. degree in electrical power engineering from the University of Saints Cyril and Methodius, Skopje, the Republic of Macedonia, in 1993 and the Ph.D. degree in electrical power engineering from the Delft University of Technology, Delft, The Netherlands, in 2002. He is also a Chevening Alumnus, and in 1997, he was an Academic Visitor with the University of Liverpool, Liverpool, U.K., where he was working with the Arc Research Group, which was working on modeling SF6 circuit breakers. His main research interests include future power systems, large-scale power system transients, intelligent protection for future power systems, and wide-area monitoring and protection. He is a Member of Cigré and actively participated in WGC4.502 and WGA2/C4.39. In 2010, he received the prestigious Dutch Hidde Nijland Prize for extraordinary research achievements. He was the recipient of the IEEE PES Prize Paper Award and the IEEE Switchgear Committee Award in 2011 and an Associate Editor for Elsevier's *International Journal of Electrical Power and Energy Systems*.

Vladimir Terzija (Fellow, IEEE) was born in Donji Baraci (former Yugoslavia). He received the Dipl.-Ing., M.Sc., and Ph.D. degrees in electrical engineering from the University of Belgrade, Belgrade, Serbia, in 1988, 1993, and 1997, respectively.

Since 2021, he has been with the Center for Energy Science and Technology, Skolkovo Institute of Science and Technology, Moscow, Russia, where he is currently a Full Professor. From 1997 to 1999, he was an Assistant Professor with the University of Belgrade, Belgrade, Serbia. From 2000 to 2006, he was a Senior Specialist of switchgear and distribution automation with ABB, Ratingen, Germany. From 2006 to 2020, he was the EPSRC Chair Professor in power system engineering with the School of Electrical and Electronic Engineering, The University of Manchester, Manchester, U.K. His current research interests include smart grid applications, wide-area monitoring, protection, and control, multienergy systems, substation automation, transient processes, ICT, data analytics, and digital signal processing applications in power systems.

He is the Editor-in-Chief of the *International Journal of Electrical Power and Energy Systems*, Alexander von Humboldt Fellow, and a DAAD and Taishan Scholar. He was the recipient of the National Friendship Award, China in 2019.

Sadegh Azizi (Senior Member, IEEE) received the B.Sc. degree in electrical power engineering from the K. N. Toosi University of Technology, Tehran, Iran, in 2007, the M.Sc. degree in electrical power engineering from the Sharif University of Technology, Tehran, Iran, in 2010, and the Ph.D. degree in electrical power engineering from the University of Tehran, Tehran, Iran, in 2016. He is currently a Lecturer in smart energy systems with the School of Electronic and Electrical Engineering, University of Leeds, Leeds, U.K. From June 2016 to January 2019, he was with The University of Manchester, Manchester, U.K., as a Postdoctoral Researcher leading their work on the protection Work Package of the EU H2020 MIGRATE project, in collaboration with more than 20 European Transmission System Operators and research institutes. He was with the Energy and System Study Center, Monenco Iran Consulting Engineers Co., Tehran, Iran, from 2009 to 2011, and the Iran Grid Management Co., Tehran, Iran, from 2013 to 2016. His research interests include wide-area monitoring, protection and control systems, digital protective relays, and applications of power electronics in power systems. He is an Associate Editor for the *International Journal of Electrical Power and Energy Systems*. He is also a Task Leader of Cigré WG B5.57, which is investigating new challenges of frequency protection in modern power systems.